IOP Conference Series: Earth and Environmental Science

PAPER • **OPEN ACCESS**

Retrograde Assemblages in the Muscovite-Biotite Gneiss of Oluyole Southwestern Nigeria, an Indication of Shear-Zone Environment

Retrograde Assemblages in the Muscovite-Biotite Gneiss of Oluyole Southwestern Nigeria, an Indication of Shear-Zone Environment

E. J. Oziegbe[1], S. A. Babarinde[1], O. Oziegbe[2] and O. T. Kayode[3]

[1] Department of Geosciences, Faculty of Science, University of Lagos, Nigeria

[2] Department of Biological Sciences, Covenant University, Nigeria
[3] Department of Physics, Covenant University, Nigeria

(eoziegbe@unilag.edu.ng, https://orcid.org/0000-0001-5772-0461; babarindesheriff@gmail.com; olubukola.oziegbe@covenantuniversity.edu.ng, https://orcid.org/0000-0001-8001-0919; olusola.kayode@covenantuniversity.edu.ng, https://orcid.org/0000-0003-4274-9151)

Corresponding email: olubukola.oziegbe@covenantuniversity.edu.ng (https://orcid.org/0000-0001-8001-0919)

Abstract. Petrographic and whole-rock geochemical study of biotite-muscovite gneiss was determined in order to interpret the metamorphic evolution of the Basement Complex of Southwestern, Nigeria. The gneiss shows a millimetric banding, and in some cases the quartzo-feldspathic bands running up to 10 cm. The gneiss has mineral assemblage biotite + plagioclase + quartz + garnet + K-feldspar + muscovite + chlorite + ilmenite ±titanite. Chlorite occurs along cleavage planes of biotite, and in some cases forms reaction rims around porphyroblasts of garnet. K-feldspar crystals are surrounded by muscovite. Titanite crystals are sub-idioblastic to xenoblastic in form, and have inclusions of ilmenite. Titanite, where present, occurs in close association with biotite and opaque minerals (ilmenite). Also, titanite forms a reaction rim around apatite. Mylonitic texture, fine-grained matrix of mica and quartz ribbons were observed. In addition, there is stretching of the quartz crystals. The SiO_2 content is greater than 60 wt %, while CaO ranges from 3.05-6.91 wt %. The M_1 foliation comprise of mineral biotite some of which are included in the opaque mineral, M_2 represents the metamorphism which gave rise to porphyroblasts of ilmenite, while the M_3 gave rise to foliations that forms a wraparound structure on the porphyroblasts of ilmenite. The last metamorphism gave rise to retrograde minerals; chlorite, titanite, and muscovite. The study suggests that this area of the Basement Complex has been subjected to multiple deformations, as well as multiple episodes of metamorphism. The structures observed are similar to those associated with shear zone environment.

Keywords: Retrograde minerals, Titanite, Reaction rim, Apatite, Mylonitic texture

1. Introduction

The Basement Complex of Nigeria lies within the Neoproterozoic to Early Paleozoic, Pan-African (ca 0.6 Ga.) province east of the West African Craton. This can be classified into three major subdivisions i.e the ancient migmatite-gneiss-quartzite complex, the schist belts and the Pan-African (ca 600 Ma.) granitic series [1]. Zircon age-dating from southeastern Nigeria, has made possible the documentation of multiple high-grade Precambrian metamorphic episodes of Pan-African and Eburnean ages. [2]. Archaean to Palaeoproterozoic age has been ascribed to migmatite–gneiss complex [3]. The migmatised gneiss of Ibadan has been reported comprise of the undifferentiated biotite-gneiss and hornblende-biotite gneiss, intercalated with amphibolite [4]. The migmatite-gneiss is a group of rock reported to have formed at Ca 2.5 Ga [5], while its migmatization occurred through the Pan African orogeny. The Basement Complex of Nigeria is reported to have undergone polyphase form of deformation during the Precambrian [6-11]. More than one episode of deformation has been reported for some gneisses in southwestern Nigeria [12-14]. Retrograde processes have been reported to be associated with fault and shear-zone environment [15], while fluids have been linked to reducing mechanisms such as the disintegration of strong minerals into weaker minerals [16-18]. The gneiss under

IOP Conf. Series: Earth and Environmental Science **1342** (2024) 012037 doi:10.1088/1755-1315/1342/1/012037

study is dissected by quartzo–feldspathic veins ranging from few centimeters to several centimeters and has been subjected to high intense folding and shearing (Figure 1). The quartzo-feldspathic veins show prominent pinkish feldspars. Even though migmatised, gneiss is the most prominent and widespread rock of the Nigerian basement [19]. In this paper, we pay close attention to the textural feature of chlorite and biotite around garnet. This paper documents retrograde as well as prograde microstructures that are present in the migmatised muscovite-biotite gneiss of Ibadan southwestern Nigeria. This study will help to deduce the possible chemical reactions that have occurred and also help to write the metamorphic evolution of rocks of the Basement Complex of Ibadan area, southwestern Nigeria.

2. Study Location

The area of study, Olonde/Aba-nla of Oluyole lies 35.9 km south of the city of Ibadan, Southwestern Nigeria (Figure 2a), which is underlain by crystalline basement rocks of variably migmatised, undifferentiated gneiss (comprising biotite, and biotite-hornblende) with intercalated amphibolite. (Figure 2b).

3. Materials and Methods

The thin sections of four gneiss samples (Figure 1c-1f) obtained from two different locations were prepared and studied at the Department of Geology, Obafemi Awolowo University laboratory in detail. Also, detailed petrography was performed at the laboratory of the Department of Geosciences, University of Lagos and photomicrographs of minerals and microstructures that are of interest were taken using a Sony digital camera. The whole rock chemical analysis was conducted at the laboratory of the Nigerian Geological Survey Agency (NGSA), Kaduna. Samples were pulverized using Retsch PM 400 planetary ball mill. The ground samples were sieved using 150 micro mesh sieves. The pulverized rock samples were then packaged for XRF (X-ray fluorescence) analysis using Energy Dispersive X-ray fluorescence spectrometer of model "Epsilon 4" by PanAlytical, Netherlands. A 20g of the prepared powdered sample was weighed each into ~~a~~ sample cup, and these cups were meticulously positioned in their designated measurement locations on the machine's sample changer. A current of 14kv was used for the major oxides, and selected filters were "kapton". Time duration measurement of 100 sec using air as the medium was employed for each sample.

4. Results and Discussion

4.1 Petrography

The following mineral assemblages were observed; biotite, chlorite, muscovite, K-feldspar, quartz, titanite, ilmenite, apatite $\pm$ epidote $\pm$ garnet. Chlorite occur along the cleavage planes of biotite with both exhibiting a preferred alignment (Figures 3 & 3b). Also, chlorite form reaction rim around prophyroblasts of garnet (Figures 3c-3f). Biotite forms reaction rims around porphyroblasts garnet (Figure 3a), some of these garnet crystals are idioblastic and elongate parallel to the foliation defined by mica (muscovite and biotite). Greenish brown biotite forms a rap around structure on porphyroblasts of opaque minerals (Figures 4a & 4b) defining an external fabric (S_e), while the porphyroblasts of opaque mineral (ilmenite) have an internal fabric (S_i) defined also by biotite (Figures 4a & 4b).

Figure 1: a) Field photohraphs showing a sheared gneiss, b) Field photograph showing gneiss with pinkish felspar, c) Hand specimen Sample C1 d) Hand specimen Sample E2, e) Hand specimen Sample C2 f) Hand specimen Sample E4

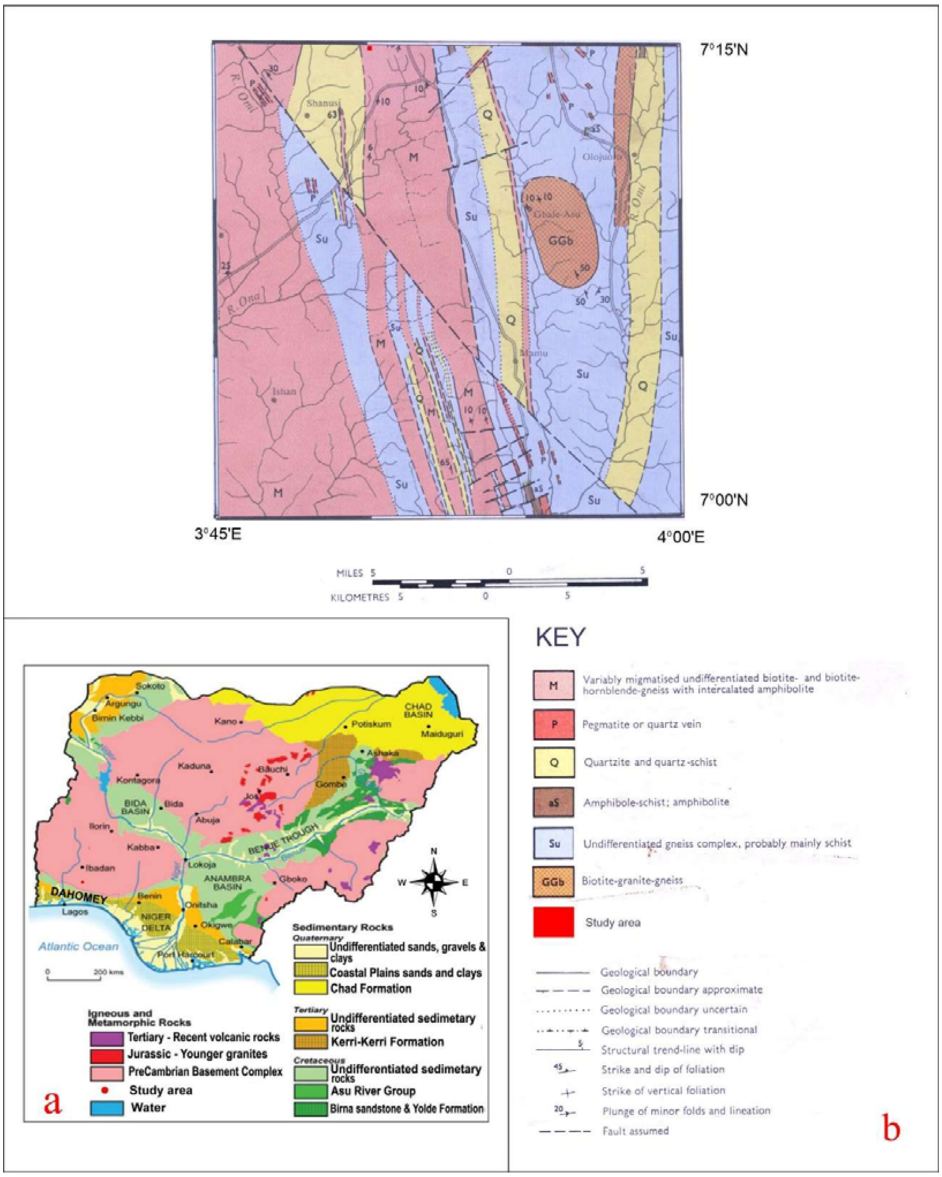

Figure 2: a) Nigeria's Geological settings which reveals that the area under study is concealed in the southwestern PreCambrian Basement Complex [20], b) Ibadan's modified geological map from GSN 1: 250,000 series sheet 59 [4]

Figure 3: Photomicrographs showing; a) chlorite (Chl) between the cleavages of biotite (Bt), chlorite (Chl) surrounding porphyroblasts of garnet (Grt) and muscovite (Ms) in contact with biotite, PPL b) muscovite (Ms) in close contact with K-feldspar (Kfs), XPL c) garnet (Grt) porphyroblasts surrounded by chlorite (Chl) and biotite (Bt), PPL d) quartz (Qtz) crystals in contact with K-feldspars (Kfs) and Muscovite (Ms), XPL e) garnet (Grt) crystals showing a breakage and elongated pattern, and in turn surrounded by muscovite (Ms), PPL f) garnet (Grt) porphyroblasts in matrix of chlorite (Chl), PPL

IOP Conf. Series: Earth and Environmental Science **1342** (2024) 012037 doi:10.1088/1755-1315/1342/1/012037

Figure 4: Photomicrographs showing; a) porphyroblasts of ilmenite (Ilm) with internal fabric surrounded by biotite (Bt) defining the external fabric, PPL b) K-feldspar (Kfs) in close contact with biotite (Bt) and muscovite (Ms), XPL c) chlorite (Chl) forming reaction rim around ilmenite (Ilm), epidote (Ep) crystal in contact with biotite (Bt), PPL d) muscovite (Ms) in contact with K-feldspar (Kfs) and epidote (Ep) XPL e) foliation defined by biotite (Bt) and muscovite (Ms), PPL f) mylotinized quartz (Qtz) showing quartz ribbons and K-feldspar (Kfs) crystals surrounded by muscovite and biotite (Bt)

Chlorite forms reaction rim on ilmenite (Figures 4c & 4d). The idioblastic to subidioblastic garnet have no inclusions of other minerals. Mica (biotite and muscovite) surround porphyroclasts of microcline. Mylonitic texture was observed, with fine-grained matrix of mica and stretching of the quartz crystals (Figure 4f). Quartz crystals were observed to exhibit undulose form of extinction. No equilibrium texture was observed between quartz crystals but rather serrated edges of quartz crystals (Figure 4f). Idioblastic crystals of apatite were observed (Figure 5).

These crystals have reaction rims of titanite around them (Figures 5a-5d). Platy crystals of apatite were observed within matrix of micas (Figures 6a & 6b). The white mica (muscovite) is closely associated with K-feldspar (Figures 6c-6e) which in some cases exhibits cross-hatched twinning. K-feldspar crystals were surrounded by xeonoblastic quartz grains (Figure 6e). There is reaction rim of titanite around ilmenite (Figures5e-5f, 6f & 7a-7d). There are inclusions of opaque (ilmenite) and apatite in xenoblastic crystals of titanite (Figure 7a & 7b). Epidote crystals were also observed in matrix of plagioclase feldspars (Figures 7e-7f).

4.2 Geochemistry

The values of the major oxides in the gneiss samples is presented in Table 1. There is a high SiO_2 contents which range from 61.22 – 67.65 wt %, Al_2O_3 14.62-15.54 wt %, high CaO of 3.05- 6.91 wt % (Table 1). Low contents of MgO 1.73-3.71 wt %, K_2O (1.73 -3.75 wt%) and TiO_2 (0.4-0.53wt %).

The rock samples (C and D) comprise amphibolite facies mineral assemblage of plagioclase, K-feldspar, quartz, biotite, muscovite, epidote, ilmenite, titanite, and garnet. The first quarry where 'C' samples were obtained has the mineral assemblage chlorite, muscovite, plagioclase, garnet, quartz and ilmenite, while the other quarry where 'E' samples were collected has the mineral assemblage, biotite, muscovite, plagioclase, quartz, titanite, epidote and ilmenite. The chlorite occurring within the cleavages of biotite and as well as around garnet can be described as late and could have resulted from retrograde processes [15,21]. Retrograde assemblages have been widely reported in the gneisses of southwestern Nigeria [15,22, 23]. In migmatites, retrograde chlorite has been reported to replace biotite along with some titanite, and retrograde muscovite occurs as lenses within matrix biotite [24]. Retrograde chlorite is a common feature in the migmatized gneiss of southwestern Nigeria [15]. The older foliation defined by biotite, may have developed at garnet-grade conditions. The dominant foliation wraps around garnet porphyroblasts and in some cases K-feldspar, and most likely crystallized during biotite-grade metamorphic conditions as presented in equation (1);

$$\text{Garnet} + \text{Biotite} + H_2O => \text{Chlorite} + \text{Muscovite} + \text{Quartz} \quad (1)$$

The retrogressive chlorite and muscovite could have developed through the above retrograde hydration reactions. Biotite cleavages are a very good pathway for fluid which facilitate retrograde process as above. Titanite and K-feldspar are typically complimentary to the biotite breakdown reaction, as are chlorite and muscovite, whose compositions are directly related to biotite composition. [25]. Granular anhedral titanite (Figures 5, 6f, 7a-7d), which can be considered a product of most reactions involving low-grade disintegration of biotite, being a main depository for Ti contained in biotite [25]. Hydration of the prograde assemblages by an influx of H_2O has been reported to produce the retrograde assemblages' chlorite–K-feldspar–muscovite–titanite [26]. Titanite are common accessory minerals in the rocks of southwestern Nigeria [27-29]. Ilmenite-titanite relationship, is a common feature in granodiorite and tonalitic rocks from southwestern Nigeria [27,28].

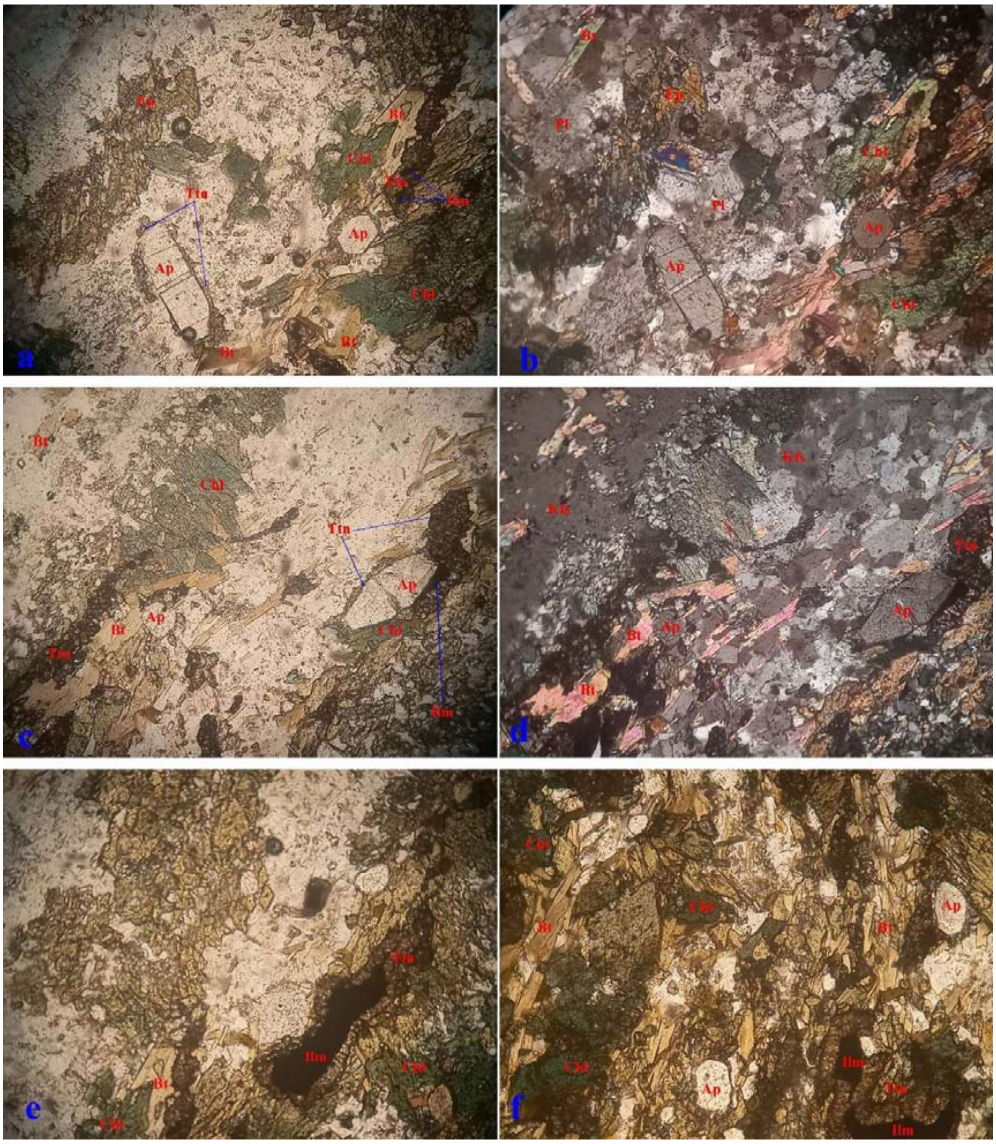

Figure 5: Photomicrographs showing; a) titanite (Ttn) forming reaction rims on idioblastic apatite (Ap), chlorite (Chl) surrounding biotite (Bt) and titanite (Ttn), PPL b) apatite (Ap) in matrix of feldspar and chlorite (Chl), PPL c) reaction rim of titanite (Ttn) on apatite (Ap), chlorite (Chl) at the edges of apatite (Ap), titanite (Ttn) and chlorite (Chl) at the edges of biotite (Bt), PPL d) apatite (Ap) in matrix of K-feldspar (Kfs) and biotite (Bt), XPL e) titanite (Ttn) forming reaction rim around ilmenite (Ilm), PPL f) apatite (Ap) in matrix of biotite (Bt) and chlorite (Chl), reaction rim of titanite (Ttn) around ilmenite (Ilm), PPL

Figure 6: Photomicrographs showing; a) platy apatite (Ap) in matrix of biotite (Bt). PPL b) apatite (Ap) surrounded by quartz (Qtz) and K-feldspar (Kfs), XPL, c) muscovite with irregular edges d) muscovite surrounded by quartz (Qtz), plagioclase (Pl) and K-feldspar (Kfs), XPL e) microcline (Mc) with cross-hatched twinning surrounded by quartz (Qtz) crystals, XPL, f) reaction rim of titanite (Ttn) around ilmenite (Ilm) PPL

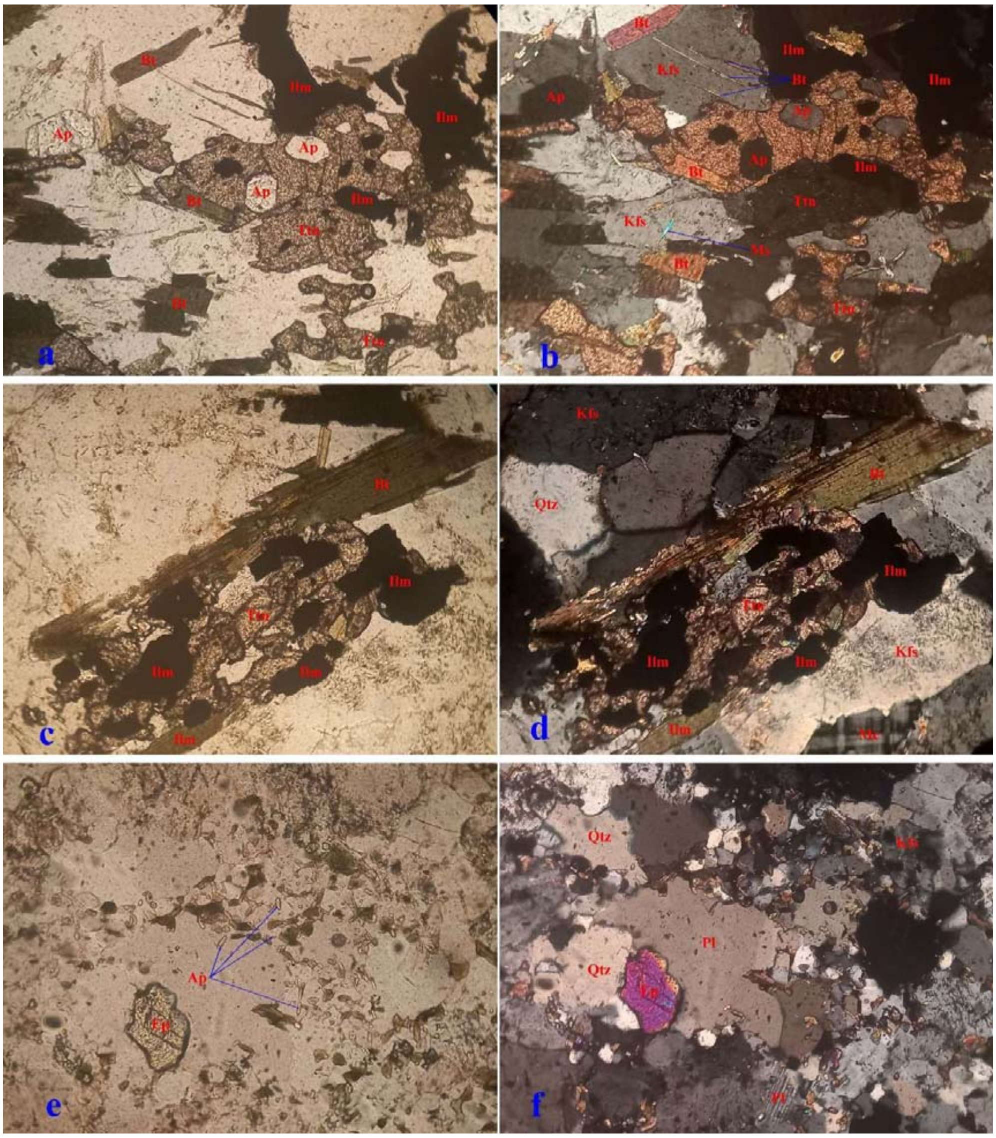

Figure 7: Photomicrographs showing; a) idioblastic apatite (Ap) and ilmenite (Ilm) occurring as inclusions in titanite (Ttn), PPL b) K-feldspar (Kfs) crystals surrounding titanite (Ttn), XPL c) ilmenite (Ilm) crystals surrounded by titanite (Ttn) and biotite (Bt), PPL d) K-feldspar and quartz (Qtz) surrounding biotite (Bt) and titanite (Ttn), microcline (Mc) showing cross-hatched twinning e) platy apatite (Ap) and xenoblastic epidote (Ep), PPL f) epidote (Ep) and apatite (Ap) in matrix of quartz and feldspars, XPL

Table 1: Whole rock chemical analysis of gneisses from Ibadan (wt %)

Samples	C1	C2	E2	E4
SiO_2	65.89	62.6	67.65	61.22
Al_2O_3	15.42	14.9	14.62	15.54
Fe_2O_3	4.03	5.22	5.62	5.66
MnO	0.05	0.08	0.06	0.1
MgO	1.73	3.71	1.99	2.22
CaO	4.3	4.44	3.05	6.91
Na_2O	3.76	3.23	ND	3.51
P_2O_3	0.39	0.44	0.53	ND
K_2O	1.73	2.45	3.75	2.18
TiO_2	0.46	0.53	0.49	0.4
L.O.I	2	2.1	1.8	2

Titanite appearing as reaction rims on ilmenite in rocks has been reported to originate from hydration reactions [30]. Titanite form retrograde reaction rim on rutile and ilmenite [31]. In prograde and retrograde reactions involving amphibolite-facies, titanite crystals can enlarge or recrystallize. [32]. The above reactions are hydration reactions which could have resulted from the infiltration of fluids during shearing. Granules of opaque surrounded by chlorite (Figure 4c) could have resulted from the breakdown of biotite which liberates Fe for the formation of ilmenite. The result of the chemical analysis (Table 1), show that there is enough aluminum to form first, feldspar, then biotite and lastly muscovite. During the retrograde process when temperature drops, Ti is released and combines with Si to form titanite. When Ca^{2+} is available from plagioclase breakdown, ilmenite is formed. The textural evidences (Figures 5, 6f, 7a-7d) suggest that titanite is of secondary origin of the breakdown of biotite;

$$\text{Ca} - \text{Plagioclase} + \text{Biotite} + 4\text{H}_2\text{O} => \text{Titanite} + \text{Ilmenite} + \text{Muscovite} \quad (2)$$

Plagioclase breaking down to give epidote, such that Ca goes into epidote and Fe goes into the formation of titanite. The presence of secondary titanite most likely indicates crystallization during isolated retrograde reactions aided by mild increase in temperature or influx of fluid [33], and is mostly caused by the degradation of biotite (Ti-bearing annite), as shown by equation (3);

$$\text{Plagioclase (An} - \text{rich)} + \text{Biotite} => \text{Titanite} + \text{Epidote} + \text{Chlorite} + \text{Quartz} \quad (3)$$

Evidence of tectonic deformation was observed on the field (Figure 3a) which showed a sheared structure. Three metamorphic events could be interpreted (M_1-M_3) from the microtextures. Two sets of foliations; S_i and S_e occur at right angles to each other. Two episodes of deformation were observed D_1 and D_2, resulting from M_1 and M_2 respectively. S_i fabric encloses biotite, an indication that there was an initial fabric formed by recrystallization M_1. D_1 can be said to produce the internal fabric S_i during M_2. The external fabric S_e can be said to be produced by D_2 during the third episode of metamorphism (M_3), thus concluding the tectono-metamorphic evolution.

5. Conclusion

Garnet can be said to be breaking down to lower grade minerals. The relative replacement of garnet is biotite > chlorite > muscovite > plagioclase > quartz. Mica crystals do not have bent cleavages which is suggestive of post-tectonism. There are two generations of biotite which define foliation (S_i & S_e). The peak mineral assemblage was garnet + chlorite + biotite + muscovite + plagioclase + quartz representing a garnet zone assemblage. All garnet crystals are retrograded either by muscovite, biotite, plagioclase, and ilmenite or chlorite. The absence of high prograde/peak assemblages in the gneiss might be as a result of prevalent deformation together with the influx of fluid. The reaction rims of titanite on apatite and ilmenite is an indication that titanite is a secondary mineral resulting from retrograde reactions.

Acknowledgment

The authors would like to recognize the Covenant University Research, Innovation, and Discovery publishing support (CUCRID).

REFERENCES

[1] EIueze, A.A. and Okunlola, O.A., 2003. Rocks of Lokoja-Jakura Schist Belt, Central Nigeria. *Journal of Minung and Geology* Vol, 39(1), pp.21-27.

[2] Ekwueme, B.N. and Kröner, A., 2006. Single zircon ages of migmatitic gneisses and granulites in the Obudu Plateau: Timing of granulite-facies metamorphism in southeastern Nigeria. *Journal of African Earth Sciences*, 44(4-5), pp.459-469. https://doi.org/10.1016/j.jafrearsci.2005.11.013

[3] Ekwueme, B.N. and Kröner, A., 1992. Preliminary zircon evaporation ages from migmatitic gneisses in Kaduna, northern Nigeria: Evidence for an early Archaean (Pre-Leonian) event in the Nigerian basement complex. *In IGCP 280 International Conference*, Salvador, Brazil.

[4] Jones, H.A. and Hockey, R.D., 1964. The geology of part of south-western Nigeria. Explanation of 1:250,000 sheets nos 59 and 68. *Bull. Geol. Surv. Nigeria*, 31, 101 PP

[5] Rahaman, M.A., 1988. Recent advances in the study of the basement complex of Nigeria. *Pre Cambrian geology of Nigeria*, pp.11-41.

[6] McCurry, P., 1976. The geology of the Precambrian to lower Paleozoic rocks of northern Nigeria -- a review. In: C.A. Kogbe (Editor), Geology of Nigeria. Elizabethan Publ. Co. Lagos, Nigeria, pp. 15--39.

[7] Grant, N.K., Hickman, M.H., Burkholder, F.R. and Powell, J.L., 1972. Kibaran metamorphic belt in Pan African domain of West Africa? *Nature*, 238: 90--91.

[8] Onyeagocha, A.C., 1984. Petrology and geologic history of NW Akwanga area in Northern Nigeria. *Journal of African Earth Sciences* (1983), 2(1), pp.41-50. https://doi.org/10.1016/0899-5362(84)90018-6

[9] Ekwueme, B.N., 1987. Structural orientations and Precambrian deformational episodes of Uwet area Oban massif, SE Nigeria. *Precambrian Research*, 34(3-4), pp.269-289. https://doi.org/10.1016/0301-9268(87)90004-0

[10] Adeoti, B. and Okonkwo, C.T., 2016. Structural geology of the basement complex rocks in Iwaraja Area, Southwestern Nigeria. *International Letters of Natural Sciences*, 58.

[11] Adedoyin, A.D., Ebiri, E.P. and Alebiosu, M.T., 2019. Deformation mechanisms, timing and shear sense analysis of part of the Precambrian terrain of southwestern Nigeria. *Journal of Fundamental and Applied Sciences*, 11(1), pp.154-172.

[12] Oyawale, A.A. and Ocan, O.O., 2020. Migmatization process and the nature of transition from amphibolite to granulite facies metamorphism in Ikare area south western Nigeria. *Journal of Geology and Mining Research*, 12(2), pp.45-64. https://doi.org/10.5897/JGMR2020.0334

[13] Oyawale, A.A., Adeoti, F.O., Ajayi, T.R. and Omitogun, A.A., 2020. Applications of remote sensing and geographic information system (GIS) in regional lineament mapping and structural analysis in Ikare Area, Southwestern Nigeria. *Journal of Geology and Mining Research*, 12(1), pp.13-24. https://doi.org/10.5897/JGMR2019.0310

[14] Oziegbe, E.J. and Oziegbe, O., 2023. Microstructural interpretation of the garnet-sillimanite-bearing granite gneiss of Ikare area, southwestern Nigeria. *Ife Journal of Science*, 25(1), pp.035-044. https://doi.org/10.4314/ijs.v25i1.5

[15] Oziegbe, E.J. and Oziegbe, O., 2023. Retrograde Assemblages of Gneisses at Arigidi and Erusu Areas of Southwestern Nigeria. *In IOP Conference Series: Earth and Environmental Science* (Vol. 1197, No. 1, p. 012010). IOP Publishing. https://doi.org/10.1088/1755-1315/1197/1/012010

[16] Oliot, E., Goncalves, P., Schulmann, K., Marquer, D. and Lexa, O., 2014. Mid-crustal shear zone formation in granitic rocks: Constraints from quantitative textural and crystallographic preferred orientations analyses. *Tectonophysics*, 612, pp.63-80. https://doi.org/10.1016/j.tecto.2013.11.032

[17] Stenvall, C.A., Fagereng, A., Diener, J.F.A., Harris, C. and Janney, P.E., 2020. Sources and effects of fluids in continental retrograde shear zones: insights from the Kuckaus Mylonite Zone, Namibia. *Geofluids*, pp.1-21. https://doi.org/10.1155/2020/3023268

[18] Putnis, A., 2021. Fluid–mineral interactions: controlling coupled mechanisms of reaction, mass transfer and deformation. *Journal of Petrology*, 62(12), p.egab092. https://doi.org/10.1093/petrology/egab092

[19] Ogezi, A.E.O., 1988. Origin and Evolution of the Basement Complex of North-Western Nigeria in the light of new Geochemical and Geochronological Data. *Precambrian Geology of Nigeria*, pp.301-312.

[20] Oladapo, O.O., Adagunodo, T.A., Aremu, A.A., Oni, O.M. and Adewoye, A.O., 2022. Evaluation of soil-gas radon concentrations from different geological units with varying strata in a crystalline basement complex of southwestern Nigeria. *Environmental Monitoring and Assessment*, 194(7), p.486. https://doi.org/10.1007/s10661-022-10173-x

[21] McWilliams, C.K., Wintsch, R.P. and Kunk, M.J., 2007. Scales of equilibrium and disequilibrium during cleavage formation in chlorite and biotite-grade phyllites, SE Vermont. *Journal of Metamorphic Geology*, 25(8), pp.895-913. https://doi.org/10.1111/j.1525-1314.2007.00734.x

[22] Oziegbe, E.J., Olarewaju, V.O., Ocan, O.O. and Costin, G., 2020. Retrogression of orthopyroxene-bearing gneiss of Iboropa Akoko, southwestern Nigeria. *Materials and Geoenvironment*, 67(3), pp.119-134. https://doi.org/10.2478/rmzmag-2020-0009

[23] Oziegbe, E.J., Ocan, O.O., Costin, G. and Horváth, P., 2021. Geochemistry and mineral chemistry of pelitic gneiss of Ikare area, southwestern Nigeria. *Heliyon*, 7(12), p.e08543. https://doi.org/10.1016/j.heliyon.2021.e08543

[24] Maki, K., Yui, T.F., Miyazaki, K., Fukuyama, M., Wang, K.L., Martens, U., Grove, M. and Liou, J.G., 2014. Petrogenesis of metatexite and diatexite migmatites determined using zircon U–Pb age, trace element and Hf isotope data, Higo metamorphic terrane, central Kyushu, Japan. *Journal of Metamorphic Geology*, 32(3), pp.301-323. https://doi.org/10.1111/jmg.12073

[25] Tulloch, A.J., 1979. Secondary Ca-Al silicates as low-grade alteration products of granitoid biotite. *Contributions to Mineralogy and Petrology*, 69, pp.105-117. https://doi.org/10.1007/BF00371854

[26] Spear, F.S. and Selverstone, J., 1983. Water exsolution from quartz: Implications for the generation of retrograde metamorphic fluids. *Geology*, 11(2), pp.82-85. https://doi.org/10.1130/0091-7613(1983)11%3C82:WEFQIF%3E2.0.CO;2

[27] Oziegbe, E. J., Oziegbe, O. and Kayode, O. T. 2023: Titanite-Ilmenite Assemblage in Granodiorite of Wasimi, Southwestern Nigeria. *Development Journal of Science and Technology Research*, Volume 12, Number 1, pp. 15-28.

[28] Oziegbe, E.J., Ocan, O.O. and Buraimoh, A.O., 2020. Petrography of Allanite-bearing Tonalite from Iwo Region, Osun State, Nigeria. *Materials and Geoenvironment*, 67(2), pp.79-89. https://doi.org/10.2478/rmzmag-2020-0006

[29] Oziegbe, E. J. and Oziegbe, O. 2023: Petrographic interpretation of Charnockitic Rocks from Osuntedo and Wasimi, Southwestern Nigeria. *Development Journal of Science and Technology Research*, Volume 12, Number 2, pp. 35-46.

[30] Harlov, D., Tropper, P., Seifert, W., Nijland, T. and Förster, H.J., 2006. Formation of Al-rich titanite (CaTiSiO4O–CaAlSiO4OH) reaction rims on ilmenite in metamorphic rocks as a function of fH2O and fO2. *Lithos*, 88(1-4), pp.72-84. https://doi.org/10.1016/j.lithos.2005.08.005

[31] Stearns, M.A., Hacker, B.R., Ratschbacher, L., Rutte, D. and Kylander-Clark, A.R.C., 2015. Titanite petrochronology of the Pamir gneiss domes: Implications for middle to deep crust exhumation and titanite closure to Pb and Zr diffusion. *Tectonics*, 34(4), pp.784-802. https://doi.org/10.1002/2014TC003774

[32] Rubatto, D. and Hermann, J., 2001. Exhumation as fast as subduction?. *Geology*, 29(1), pp.3-6. https://doi.org/10.1130/0091-7613(2001)029%3C0003:EAFAS%3E2.0.CO;2

[33] Corfu, F. and Stone, D., 1998. The significance of titanite and apatite U-Pb ages: constraints for the post-magmatic thermal-hydrothermal evolution of a batholithic complex, Berens River area, northwestern Superior Province, Canada. *Geochimica et Cosmochimica Acta*, 62(17), pp.2979-2995. https://doi.org/10.1016/S0016-7037(98)00225-7